J. Fluid Mech. (2005), *vol.* 545, *pp.* 271–280.
doi:10.1017/S0022112005006944 Printed in the United Kingdom

Spreading of a drop of neutrally buoyant suspension

By MAXIME NICOLAS

Groupe Écoulements de Particules, Institut Universitaire des Systèmes Thermiques Industriels, UMR 6595 CNRS-Université de Provence, 5 rue Fermi, 13453 Marseille cedex 13, France

(Received 1 February 2005 and in revised form 8 July 2005)

The spreading of suspension drops on a flat surface is studied using mixtures of liquid and density-matched particles. As expected from an energy balance model, the spreading factor is reduced with increasing particle volume fraction. This decrease is quantitatively understood through an effective viscosity coefficient. However, for large drop Reynolds number, the particles are not uniformly distributed into a spread drop but form an annulus. For higher impact velocities, a particle-induced break-up of the drop is observed.

1. Introduction

A great number of industrial processes rely on the understanding of the mechanics of the impact and spreading of liquid drops on a flat substrate. Since the pioneering work of Worthington, there have been numerous studies of drop spreading phenomena (see Rein 1993 for a review). Most of the studies, including viscous spreading models (Gu & Li 1998, 2000), are based on an energy balance model (presented in § 2). Considering a drop of diameter d_0 impacting with a velocity U on a flat surface, the spreading diameter βd_0 is predicted to depend on the Reynolds number $Re_0 = \rho d_0 U/\eta$ and the Weber number $We = \rho d_0 U^2/\sigma$ (ρ is the density of the liquid, η its dynamic viscosity and σ is the interfacial tension of the liquid with air). In the limit of a vanishing impact velocity, the spreading factor β depends only on the contact angle and the Bond number $Bo = \rho g d_0^2/\sigma$ (Shikhmurzaev 1997; Reznik & Yarin 2002). For a moderate impact velocity, the kinetic energy is dissipated by viscous forces and the drop reaches a static state after a finite spreading time. Some fingering patterns of the contact line may occur during this process (Thoroddsen & Sakakibara 1998). If the initial kinetic energy is too large to be dissipated by viscosity, splashing of the drop occurs.

Range & Feuillebois (1998) have shown that the value of the Reynolds number Re_0 at which splashing is first observed is strongly affected by the roughness of the plane on which the drops impinges. Moreover, when the Ohnesorge number $Oh = \sqrt{We}/Re_0$ is small, the viscosity is negligible and the critical Re_0 was found to be inversely proportional to Oh, with the constant of proportionality depending only on the roughness of the plate. At larger Oh, according to Stow & Hadfield (1981) and Mundo, Sommerfeld & Tropea (1995), this critical Re_0 becomes inversely proportional to $Oh^{0.8}$. This criterion can also be written as $We^{0.5} Re_0^{0.25} > K_0$, where K_0 is a constant depending on the surface roughness.

To date there has been no quantitative study of the deposition of a drop of suspension. However, some industrial processes use a mixture of a liquid solvent and

solid particles instead of a pure liquid. For example, an emerging application such as a particle-laden ink jet requires small-volume droplets of suspension impacting at high velocity (Seerden *et al.* 2001). Since this small-scale and fast-time phenomenon is quite difficult to observe, a scaled experiment should help to understand the influence of non-deformable solids on the drop spreading. We aim to describe the spreading of a particle-laden drop impacting on a flat surface. The suspension is made of particles with diameter d_p and density equal to that of the liquid. Assuming that the particles are initially uniformly distributed in the drop volume with a particle volume fraction ϕ, the drop viscosity $\eta\eta_r(\phi)$ can be estimated using an effective viscosity model such as the Krieger–Dougherty correlation. The relevant Reynolds number is thus modified and is written $Re = Re_0/\eta_r(\phi)$.

Our goal is to obtain some insight into the particle-laden drop impact phenomenon. A predictive model for the effect of the particles on the spreading factor is proposed and compared with experimental results. In our experiment we measure the spreading factor and the particle position distribution in the spread drop. Two particle configurations are observed: a uniform distribution for low Re_0 and annular distribution for higher Re_0. A qualitative analysis is suggested. For a high impact velocity, break-up of the suspension drop may occur and can be described by a $We^{0.5}Re_0^{0.25} > K_0$ criterion. But unexpectedly, K_0 is seen to decrease when the particle volume fraction is increased.

2. Theoretical predictions

2.1. *Mass and energy balance model*

The spreading process involves inertial, viscous and gravity forces, the interfacial tension and the wettability of the liquid on the solid surface. Despite this large number of parameters, some predictions can be made using mass conservation and energy balance equations.

The first conservation equation is the mass or volume conservation. Whatever the shape of the spread drop (a flat disk or a spherical cap), its volume must be equal to the volume $\pi d_0^3/6$ of the spherical drop before impacting on the plane.

The second equation is a balance between energy before the impact and energy when the spreading is over. This is written

$$E_k + E_p + E_s = E_k' + E_p' + E_s' + W_d \tag{2.1}$$

where indices k, p and s denote kinetic, potential and surface energies respectively. The work of viscous dissipative forces during the spreading is W_d. The initial kinetic energy is $E_k = \frac{1}{12}\pi\rho d_0^3 U^2$. After the spreading, the kinetic energy is zero: $E_k' = 0$. For high-velocity drop impacts (i.e. $Re \gg 1$ and $We \gg 1$), since the kinetic energy overcomes the potential and surface energies, it is only balanced by the work of dissipative viscous forces.

The energy dissipated by viscous forces is commonly estimated as $\int_0^{t_s}\int_{\Omega} \Phi \,\mathrm{d}\,\Omega \mathrm{d}t$ where t_s is the time of spreading and Ω the volume of the drop. The spreading time t_s scales as d_0/U and Pasandideh-Fard *et al.* (1996) suggested $t_s = (8/3)(d_0/U)$ as a correct value. The volumic rate of dissipated energy Φ then scales as $\alpha\eta(U/L)^2$ with L the typical length over which the velocity varies and α a dimensionless number. Although this number may vary a little with the Reynolds number, we choose to keep it constant for simplicity. For high-viscosity liquids, viscous dissipation occurs in the whole drop volume and the mean thickness of the spread drop is $L = h = 2d_0/3\beta^2$ (Chandra & Avedisian 1991; Mao, Kuhn & Honghi 1997; Park *et al.* 2003). The energy

	ρ (g cm^{-3})	η (g cm^{-1})	σ (mN m^{-1})	Material	d_p (μm)	d_0 (mm)	d_0/d_p
L1P1	1.18 ± 0.1	0.22 ± 0.01	56.8 ± 0.5	PMMA	636 ± 24	4.7 ± 0.2	7.4 ± 0.5
L2P2	1.05 ± 0.005	0.011 ± 0.001	28.0 ± 0.4	polystyrene	720 ± 37	4.0 ± 0.2	5.5 ± 0.3
L2P3	1.05 ± 0.005	0.011 ± 0.001	28.0 ± 0.4	polystyrene	381 ± 39	4.4 ± 0.1	10.5 ± 1

TABLE 1. Characteristics of liquid, particles and drops of suspension.

dissipated by viscosity is then $W_d = \alpha\pi\eta U d_0^2 \beta^4$ and the energy balance equation (2.1) leads to

$$\beta = \left(\frac{Re}{12\alpha}\right)^{1/4}. \tag{2.2}$$

2.2. *Effect of the particles on the spreading*

The effective viscosity of a suspension is known to be larger than the viscosity of the liquid alone. This increase has been the subject of numerous studies since Einstein in 1905 and the effective viscosity of a suspension is formally written as $\eta_s = \eta_f \eta_r(\phi)$ where $\eta_r(\phi)$ is a monotonic function of the particle fraction. For a wide range of particle volume fraction, the Krieger–Dougherty model estimates the relative viscosity as $\eta_r = (1 - \phi/\phi_m)^{-n}$ where $\phi_m = 0.68$ is the random close packing volume fraction and $n = 1.87$. As stated in the introduction, the particle-laden drop Reynolds number is $Re_0/\eta_r(\phi)$, and assuming that (2.2) is valid, one should expect a spreading factor

$$\beta = \left(\frac{Re_0}{12\alpha}\right)^{1/4} \left(1 - \frac{\phi}{\phi_m}\right)^{n/4}. \tag{2.3}$$

And if we assume that the volume fraction is low ($\phi \ll \phi_m$), then

$$\beta \approx \left(\frac{Re_0}{12\alpha}\right)^{1/4} \left(1 - \frac{n}{4}\frac{\phi}{\phi_m}\right) \tag{2.4}$$

and the decrease of spreading due to particles is

$$\frac{\mathrm{d}\beta}{\mathrm{d}\phi} = -\frac{n}{4\phi_m}\left(\frac{Re_0}{12\alpha}\right)^{1/4} \tag{2.5}$$

which gives $\mathrm{d}\beta/\mathrm{d}\phi = -0.37 Re_0^{1/4}$ for $\alpha = 1$. This expression is compared to experiments in § 4.1.

3. Materials and experimental conditions

We used different liquids and particles to prepare the density-matched suspensions (see table 1). Liquid L1 was a water and glycerol mixture and liquid L2 was salted water. A small amount of surfactant (a liquid soap) was added to L2 to prevent particle aggregation. Both liquids were dyed using fluoresceine. Viscosity η was measured using a Rheomat RM 180 Couette rheometer and a Gilmont falling ball viscosimeter. Surface tension was measured with a ring tensiometer. All experiments and measurements were carried at $T = 23\,^{\circ}\mathrm{C}$. When needed, pure liquid drop impacts were studied.

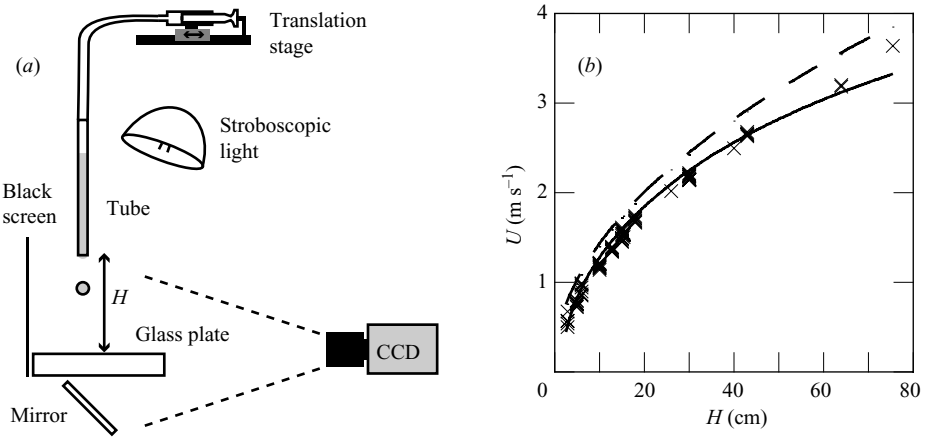

FIGURE 1. (*a*) Schematic diagram of the experimental apparatus. (*b*) Correlation between the height of release H and the impact velocity U. The dashed line is the free-fall velocity and the continuous line is the velocity obtained with $U = \sqrt{gH_0(1 - \exp(-2(H - \Delta H)/H_0)}$.

Figure 1(*a*) shows the experimental apparatus used to produce droplets at the outlet of a cylindrical tube and to photograph their fall and impact on a clean plate of glass at a distance H below. A 45° mirror placed below the glass plate was used to photograph the spreading while the CCD camera was focused on the vertical plane below the tube. A stroboscopic light produced 100 to 175 flashes per second while the camera shutter rate was 25 Hz. The flash duration was short enough to freeze the droplet motion during the fall or the spreading. A fast camera (1000 frames s^{-1}) was also used to record the fast motion and the particle positions during the spreading.

Delivery of a single droplet was ensured by a home-made programmable pump based on a translation stage driven by a PC computer through a LabView interface. The tube had a 3 mm inner diameter and was 200 mm long. The velocity U of each droplet was measured between two successive snapshots just before the impact. The measured impact velocity was seen to be slightly different from the free-fall velocity $\sqrt{2gH}$ (see figure 1*b*). Since the droplet is larger than the capillary length, the droplet is not perfectly spherical and exhibits oscillations during the fall. Since the drag is not negligible, we assume a constant friction coefficient C_f (as suggested by Range & Feuillebois 1998), hence the impact velocity is $U = \sqrt{gH_0(1 - \exp(-2(H - \Delta H)/H_0)}$ where ΔH is the distance between the tube and the droplet at zero velocity, and $H_0 = 4\rho d_0/(3C_f\rho_{air})$, in good agreement with the experimental results (see figure 1*b*).

Once the droplet is spread on the glass plate, we computed the spreading factor $\beta = \sqrt{2A_w/\pi d_0^2}$ by measuring the wetted area A_w on the image. If break-up of the drop occurred, the spreading factor was measured as the maximum diameter of the wetted area divided by d_0. For each experiment, we measured the initial drop diameter d_0, the spreading factor β, the number of particles N, the particle volume fraction $\phi = N(d_p/d_0)^3$ and the positions of each particle. We define $r = 2\sqrt{x^2 + y^2}/\beta d_0$ the dimensionless particle distance from the centre of impact.

In our experiments, the particle volume fraction was varied from 0 (pure liquid) to 0.45, leading to an effective viscosity $1 < \eta_r < 7.45$. The distance H between the tube and the glass plate was varied from 2.9 to 75.5 cm. The Reynolds number range was $79 < Re < 9907$, the Weber number was $24 < We < 1276$, the Ohnesorge number was $0.003 < Oh < 0.11$. and the Bond number was $3.5 < Bo < 8.0$.

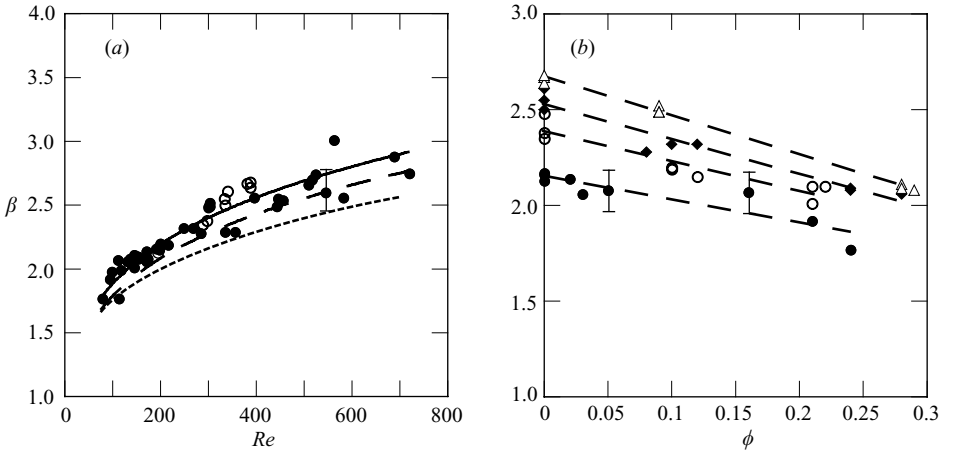

FIGURE 2. (*a*) Spreading factor vs. $Re = Re_0/\eta_r$ for pure liquid L1 (open circles) and suspension L1P1 (filled circles). Dotted line is the prediction due to Pasandideh-Fard *et al.* (1996), dashed line is (2.2) with $\alpha = 1$, and solid line is (2.2) with $\alpha = 0.89$. (*b*) Effect of the particle volume fraction on the spreading factor: $Re_0 = 188$ (filled circles), $Re_0 = 292$ (open circles), $Re_0 = 348$ (filled diamonds) and $Re_0 = 389$ (open triangles) for the suspension L1P1. The dashed lines are the best linear trends for each set of data.

4. Results

4.1. *Spreading factor and transition to a break-up regime*

Experiments with the most viscous liquid L1 were done with impact velocities ranging from 0.5 to 3.64 m s^{-1}. The particle volume fraction was up to 30 %. No drop break-up was observed for these ranges of parameters. The average value of $Re/81\beta^4$ is 0.11 ± 0.02, suggesting that viscous dissipation occurs in the whole volume of the drop. We compare in figure 2(*a*) our measurements with the spreading factor predicted by (2.2), and the prediction made by Pasandideh-Fard *et al.* (1996). The spreading factor ranges from 1.5 to 3 for a Reynolds number varying from 100 to 700. The model is in good agreement with the experimental results if the fitting parameter α is 0.89 (solid line). For comparison, the theoretical spreading factor is shown for $\alpha = 1$ (dotted line). This good agreement shows that the effective viscosity approach still holds even if the liquid film thickness h is smaller than the particle diameter d_p. This occurs as soon as the spreading factor β is larger than $\sqrt{2d_0/3d_p}$ which takes the value 2.2 for experiments L1P1. As expected, an increase in volume fraction increases the effective viscosity of the suspension and thus decreases the spreading factor. This trend is shown in figure 2(*b*) where we present four sets of results corresponding to four impact velocities. The error bars give an estimate of the experimental error in the spreading factor measurements. The decrease of β can be fitted well by a linear function, allowing measurement of $\mathrm{d}\beta/\mathrm{d}\phi$.

Results for the less viscous liquid (L2) are shown on figure 3. A first comment is that the size of the particles does not seem to play a strong role in the spreading. Secondly, β varies from 2 to 5 for a Reynolds number increasing from 500 to 10000. The agreement of experimental results with the β predicted by (2.2) is fairly good but the data show more scatter than those for the more viscous suspension. Nevertheless, we still observe a decrease of β with the particle volume fraction the (figure 3*b*), and $\mathrm{d}\beta/\mathrm{d}\phi$ can still be measured using a linear fit to the experimental data.

The decrease of the spreading factor due to particles $\mathrm{d}\beta/\mathrm{d}\phi$ is plotted in figure 4(*a*) and compared to the value predicted by (2.5). The results for all the particle/fluid

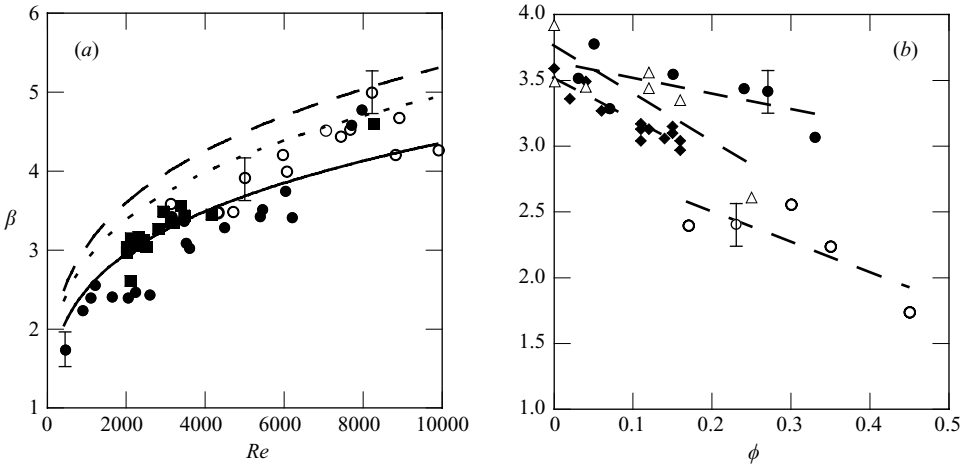

FIGURE 3. (*a*) Spreading factor vs. $Re = Re_0/\eta_r$ for pure liquid L2 (open circles), and suspensions L2P2 (filled squares) and L2P3 (filled circles). Solid line is the (2.2) for $\alpha = 1.57$, dashed line computed with $\alpha = 1$ and dotted line is computed with the expression given by Pasandideh-Fard *et al.* (1996). (*b*) Effect of particle volume fraction on the spreading factor: suspension L2P2 at $Re_0 = 3496$ (open circles) and $Re_0 = 6118$ (filled circles); suspension L2P3 at $Re_0 = 3326$ (diamonds) and $Re_0 = 4917$ (triangles). The dashed lines are the best linear trends for each set of data.

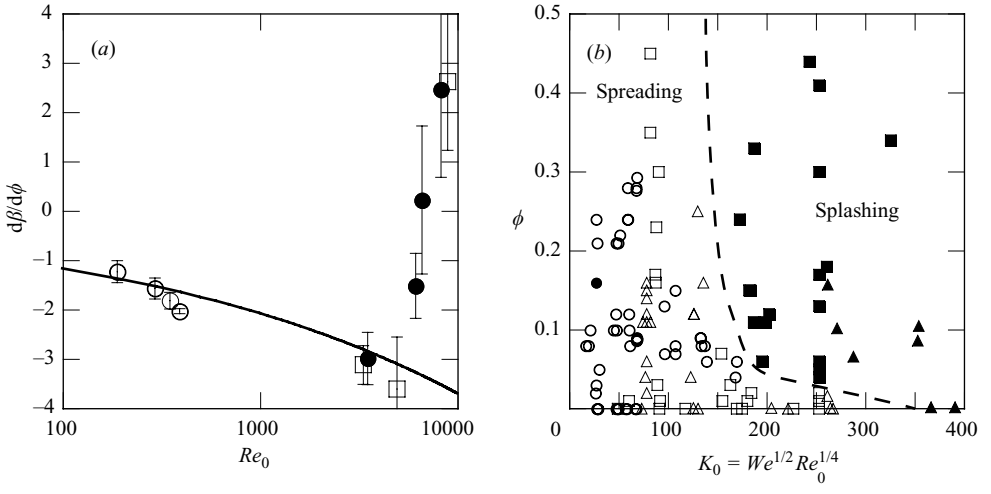

FIGURE 4. (*a*) Spreading reduction due to the particles L1P1 (open circles), L2P2 (filled circles) and L2P3 (squares). The continuous line is (2.5) computed with $\phi_m = 0.68$, $n = 1.87$ and $\alpha = 1$. (*b*) Map of the spreading/splashing regimes in the (K_0, ϕ)-plane: L1P1 (circles), L2P2 (squares) and L2P3 (triangles).

combinations follow the same curve. Despite the scattering of the experimental data for the viscous liquid L2, it shows a good agreement for $Re_0 < 5000$: $d\beta/d\phi$ is negative and scales as $Re_0^{1/4}$. For $Re_0 > 5000$, $d\beta/d\phi$ increases and eventually becomes positive for $Re_0 \gtrsim 6000$. In that range of Reynolds number, the particles do not reduce the spreading compared to the pure liquid impact, but on the contrary enhance the spreading. The resulting impact is no longer a circular contact line, but a rather distorted line or even several droplets formed by the break-up of the impacting drop.

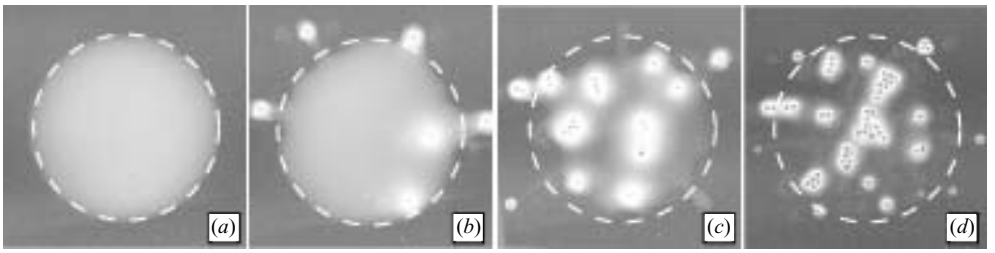

FIGURE 5. Photographs of droplets impacting at the same velocity $U = 2.15\,\mathrm{m\,s^{-1}}$: (*a*) Liquid L2 without particles (*b*) Liquid L2 without particles at $\phi = 0.04$, (*c*) $\phi = 0.13$ and (*d*) $\phi = 0.30$. Pure liquid Reynolds number is $Re_0 = 8217$.

An example of such a break-up is shown on figure 5. The four photographs depict the effect of an increase of ϕ on the impact of a L2P2 suspension drop for the same $Re_0 = 8217$. Some particles are found outside the circle depicting the pure-liquid spread drop. In some cases, some particles were observed to move far from the impact point and eventually to leave the glass plate. All our observations are summarized in figure 4(*b*). Following Mundo *et al.* (1995), we attempt to describe the break-up regime using a critical number $K_0 = We^{0.5} Re_0^{0.25}$. This critical number seems to depend on the volume fraction: when ϕ increases, K_0 is unexpectedly decreased. This is in apparent contradiction with the energy balance model.

Finally, one can observe that the particles in the spread drop are grouped in clusters. This is due to surface tension effects because the liquid film thickness h is lower than the particle diameter. The particles deform the liquid/air interface and increase its surface energy. This is very similar to what happens in a raft of floating bubbles (Bragg & Nye 1947), where the interaction between two bubbles can be described by a potential analogue to the interaction potential between two atoms (Shi & Argon 1982). The attractive force between two particles at a liquid–gas interface has also been studied by Joseph *et al.* (2003).

4.2. *Particle distribution in the spread drop*

For each experiment we measured the dimensionless radial particle positions r and computed the probability $P_r(r)$ for a particle to be at a distance r from the spread drop centre. The probability density function (p.d.f.) of the position is $P(r, \theta)$ and must satisfy $\pi^{-1} \int_0^{2\pi} \int_0^1 P(r, \theta) r \, \mathrm{d}\theta \, \mathrm{d}r = 1$. Assuming that the spreading is axisymetric, P does not depend upon θ, and $P = P_r/2r$. The maximum value of the p.d.f. $P(r)$ denotes the preferred position for the particles in the spread drop.

We show on figure 6(*a*, *b*) the particle positions and the probability P for the suspension L1P1 for a Reynolds number $Re_0 < 807$. The probability has a weak maximum for $r < 0.1$ and is nearly constant for $0.1 < r < 0.7$. As can be seen on figure 6(*a*) the particles seem randomly dispersed in a disk of radius $r \approx 0.7$. The probability density decreases strongly for $r > 0.7$ which is the signature of a depletion of particles near the boundary of the droplet.

The situation is quite different for suspensions made with a less viscous liquid. Figure 6(*c*, *d*) shows the particle positions and the p.d.f. for drops L2P3 with $Re_0 \approx 3350$. The maximum of the p.d.f. is for a radius $0.4 < r < 0.5$ and the depletion of particles occurs in the centre of the droplet ($r < 0.2$) as well as in the outer annulus ($r > 0.7$). This situation was also observed for higher Reynolds numbers ($Re_0 \approx 5000$) as well for the drops of suspension L2P2. Whatever the liquid and the particles,

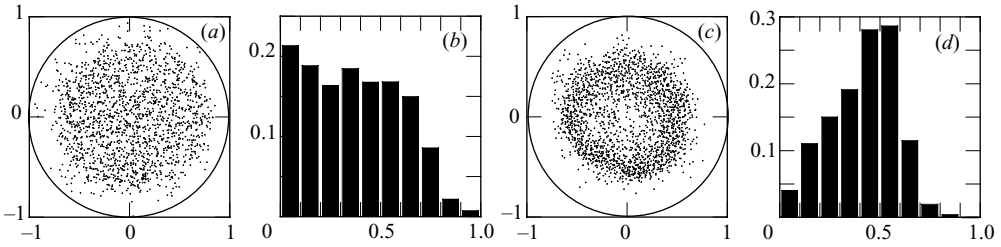

FIGURE 6. (*a*) Particle position distribution in the spread droplet and (*b*) radial probability P for L1P1, $140 < Re_0 < 807$ and $0.03 < \phi < 0.28$. (*c*) Particle position distribution in the spread droplet and (*d*) radial probability P for L2P3, $3184 < Re_0 < 3513$ and $0.11 < \phi < 0.16$. Data were collected from different runs.

it seems that there is no obvious dependence of the position distribution upon the particle volume fraction.

The annular distribution of particles for Reynolds numbers larger than 3000 may be explained by the oscillation of the liquid during the spreading. If the spreading is governed by viscous forces (low Re_0), all the momentum of the liquid is dissipated during the time needed to reach a steady contact line between the drop and the solid substrate. Conversely, if inertial forces are large enough, a fraction of momentum may remain after the contact line motion has stopped. A raised rim then forms at the periphery and the central liquid pool thins out. The rim is then pulled back towards the centre since the interfacial tension minimizes the liquid/air contact area. We suggest that the particles follow the liquid oscillations qualitatively, as they are density matched with the liquid. Moreover, if the local thickness of the liquid is lower than the particle diameter d_p, the interface is deformed and its motion may create a force acting on the particle. In the same manner, the periphery of the drop has a very low thickness and this prevents the particles getting close to the contact line, creating a depletion of particles for large r values ($r > 0.7$ from our results).

This assumption has been checked with the video recording large frame rate (1000 f.p.s.) of a drop spreading for a Reynolds number at which the annular distribution of particles occurs. We show on figure 7 the time evolution of the spreading factor $\beta(t)$ and the motion of one test particle on the same time scale. While the drop contact line stops growing 7 ms after the impact, the test particle still moves, reaches a maximum radial position at $t = 19$ ms, and then moves back to reach a steady position at $t = 48$ ms. The particles are thus observed to move after the spreading factor has reached a constant value.

5. Conclusion

We have studied the impact, spreading and break-up of a liquid drop containing solid density-matched particles. Using an effective viscosity model for the drop, the spreading factor scales as $Re^{1/4}$, and the effect of solid particles is quantitatively described. A uniform particle distribution in the spread drop is observed for $Re \lesssim 800$ and an annular distribution is observed for larger values of the Reynolds number. The periphery of the drop is always depleted of particles owing to interfacial forces acting on the particles. For a large impact velocity, break-up of the drop is observed. The break-up criterion takes the form $We^{1/2}Re_0^{1/4} > K_0(\phi)$ where K_0 decreasing when ϕ increases.

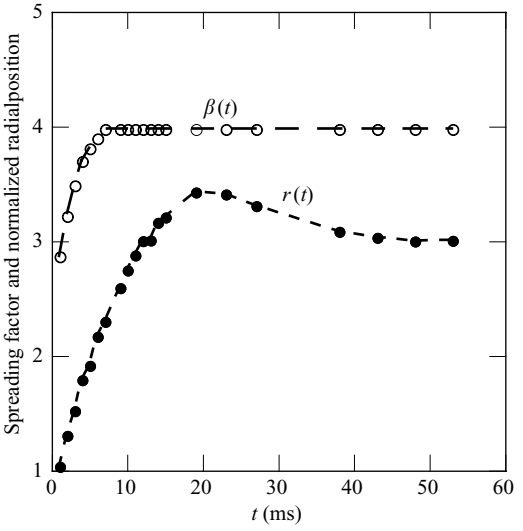

FIGURE 7. Time evolution of the spreading factor $\beta(t)$ (open circles) compared to the normalized radial position of a test particle (filled circles) for suspension L2P2. The Reynolds number was $Re_0 = 6500$ and the particle volume fraction was $\phi = 0.02$.

Some clusters of particles were also observed for the less viscous liquid. This feature demonstrates the interaction of the particles with the liquid/air interface, and this issue is surely connected with the unexpected transition from the spreading to the break-up regime. This might suggest a further study of the forces and stresses between a particle and an interface.

The author thanks É. Guazzelli for discussions and help.

REFERENCES

BRAGG, L. & NYE, J. F. 1947 A dynamical model of a crystal structure. *Proc. R. Soc. Lond.* **190**, 474–481.

CHANDRA, S. & AVEDISIAN, C. T. 1991 On the collision of a droplet with a solid surface. *Proc. R. Soc. Lond.* A **432**, 13–41.

FORD, R. E. & FURMIDGE, C. G. L. 1967 Impact and spreading of spray drops on foliar surfaces. *Wetting Soc. Chem. Industry Monograph*, pp. 417–432.

GU, Y. & LI, D. 1998 A model for a liquid drop spreading on a solid surface. *Colloids Surface* A **142**, 243–256.

GU, Y. & LI, D. 2000 Liquid drop spreading on solid surfaces at low impact speeds. *Colloids Surface* A **163**, 239–245.

JOSEPH, D. D., WANG, J., BAI, R., YANG, B. H. & HU, H. H. 2003 Particle motion in a liquid film rimming the inside of a partially filled rotating cylinder. *J. Fluid Mech.* **496**, 139–163.

MAO, T., KUHN, D. C. S. & HONGHI, T. 1997 Spread an rebound of liquid droplets upon impact on flat surfaces. *AIChE J.* **43**, 2169–2179.

MUNDO, C., SOMMERFELD, M. & TROPEA, C. 1995 Droplet-wall collisions: experimental studies of the deformation and breakup process. *Intl J. Multiphase Flow* **21**, 151–173.

PARK, H., CARR, W. W., ZHU, J. & MORRIS, J. F. 2003 Single drop impaction on a solid surface. *AIChE J.* **49**, 2461–2471.

PASANDIDEH-FARD, M., QIAO, Y. M., CHANDRA, S. & MOSTAGHIMI, I. 1996 Capillary effects during droplet impact on a solid surface. *Phys. Fluids* **8**, 650–659.

RANGE, K. & FEUILLEBOIS, F. 1998 Influence of surface roughness on liquid drop impact. *J. Colloid Interface Sci.* **203**, 16–30.

Rein, M. 1993 Phenomena of liquid drop impact on solid and liquid surfaces. *Fluid Dyn. Res.* **12**, 61–93.

Reznik, S. N. & Yarin, A. L. 2002 Spreading of an axisymmetric viscous drop due to gravity and capillarity on a dry horizontal wall. *Intl J. Multiphase Flow* **28**, 1437–1457.

Seerden, K. A. M., Reis, N., Evans, J. R. G., Grant, P. S., Halloran, J. W. & Derby, B. 2001 Ink-jet printing of wax-based alumina suspensions. *J. Am. Ceram. Soc.* **34**, 2514–2520.

Shi, L. T. & Argon, A. S. 1982 The potential and force law between different-size bubbles in soap bubble raft. *Phil. Mag* A **46**(2), 255–274.

Shikhmurzaev, Y. D. 1997 Spreading of drops on solid surfaces in a quasi-static regime. *Phys. Fluids* **9**, 266–275.

Stow, C. D. & Hadfield, M. G. 1981 An experimental investigation on fluid flow resulting from the impact of a water drop with an unyielding dry surface. *Proc. R. Soc. Lond.* A **373**, 419.

Thoroddsen, S. T. & Sakakibara, J. 1998 Evolution of the fingering pattern of an impacting drop. *Phys. Fluids* **10**, 1359–1374.